Excitability in a Quantum Dot Semiconductor Laser with Optical Injection

D. Goulding,[1,3] S. P. Hegarty,[1] O. Rasskazov,[1,2] S. Melnik,[1,3] M. Hartnett,[1,3] G. Greene,[1] J. G. McInerney,[1,3] D. Rachinskii,[4] and G. Huyet[1,2]

[1]*Tyndall National Institute, Lee Maltings, Cork, Ireland*
[2]*Department of Applied Physics and Instrumentation, Cork Institute of Technology, Cork, Ireland*
[3]*Physics Department, National University of Ireland, University College Cork, Ireland*
[4]*Department of Applied Mathematics, University College, Cork, Ireland*

(Received 31 July 2006; published 10 April 2007)

We experimentally analyze the dynamics of a quantum dot semiconductor laser operating under optical injection. We observe the appearance of single- and double-pulse excitability at one boundary of the locking region. Theoretical considerations show that these pulses are related to a saddle-node bifurcation on a limit cycle as in the Adler equation. The double pulses are related to a period-doubling bifurcation and occur on the same homoclinic curve as the single pulses.

DOI: 10.1103/PhysRevLett.98.153903 PACS numbers: 42.65.Sf, 05.45.−a, 42.55.Px

Synchronization is one of the most elegant phenomena of nonlinear dynamics and is manifest in many systems in biology, medicine, science, and engineering. The modern study of synchronization [1] was begun by Huygens who noted that two wall clocks of different natural frequencies synchronized when attached to the same wall. This phenomenon lay unexplained until the development of nonlinear dynamics by Poincaré and the first in depth examination of forced oscillators was made by van der Pol. Synchronization between electrical oscillators was demonstrated by Adler [2] who developed a mechanical model analogy for the system. Adler's model allowed two different transients to the stable steady state with very different trajectories in phase space, an important insight for the future understanding of excitability.

Excitability was originally coined in the analysis of the action potential of the axon of the giant Atlantic squid [3] but it is now commonly used to describe any stable dynamical system that exhibits pulses when perturbed above a certain threshold level [4]. The pulses are evidence of a large excursion in the phase space of the system. Once a pulse has been created, a refractory period of time must follow before another excitation of the system is possible. With this definition, excitability is observed in many experiments including nonlinear chemical reactions, ion channel firing, and climate dynamics. In spatially extended dynamical systems, excitability usually leads to the appearance of wave fronts and spiral waves that are at the origin of tachycardia [4]. It was also noted that excitability could be observed in various optical systems including lasers with saturable absorbers [5], semiconductor lasers with optical feedback [6], and multisection lasers [7].

The dynamics of lasers under optical injection from a single frequency master laser has been the subject of many studies to generate optical bistability [8] to increase the modulation bandwidth of semiconductor lasers [9], to create spatial solitons [10], and to study instabilities in nonlinear dynamical systems [11]. It has also been suggested that this experiment might be an excellent prototype to observe optical excitability [12] since the phase dynamics is described by the Adler equation. In this equation, the locking or unlocking bifurcation is described by a saddle-node bifurcation on a limit cycle. More recent analyses of semiconductor laser rate equations with optical injection have also shown the possibility of observing multipulse excitability associated with n-homoclinic bifurcations [13]. Although excitability has been observed experimentally in several laser systems [5–7], there is not yet any experimental evidence of excitability in a laser with optical injection. One possible explanation for this absence is that previous studies have been carried out with bulk or quantum well semiconductor lasers and the weakly damped relaxation oscillations characteristic of these lasers become quickly self-sustained and chaotic for moderate optical injection, thus reducing the observable range of optical excitability.

Recent progress in semiconductor growth technology has led to the realization of quantum dot (QD) semiconductor lasers. In these devices, the electron wave function is confined in three dimensions leading to some distinctive features, including strongly damped relaxation oscillations that inhibit the onset of instabilities induced by optical feedback [14]. Here, we present the first study of nonlinear dynamics in a highly damped QD semiconductor laser under optical injection. We find that the QD laser can stably synchronize with the master laser over a significant detuning range. At one boundary only of the locking region we observe complex behavior including single excitable pulses, double excitable pulses, and random switching between locked and unlocked states.

The experiment was carried out on samples of 1.5 mm long InAs QD lasers, as described in [15]. The laser was mounted on a temperature controlled stage with optical access to both facets. The laser threshold was 37 mA and the slope efficiency was 0.04 mW/mA. The master laser was a commercial external cavity tunable device with linewidth <100 kHz and tunable in steps of 0.1 pm. The master output was guided in a polarization maintaining

 © 2007 The American Physical Society

fiber and coupled into the slave waveguide using a pair of matched aspheric lenses. Optical isolators were used to prevent optical feedback in the system and temperature stability was critical in order to prevent unwanted variations in the master-slave detuning. The slave laser output was coupled to an optical spectrum analyzer or to a 12 GHz photodiode, which was either connected directly to a real-time oscilloscope of 6 GHz bandwidth or amplified and connected to an electrical spectrum analyzer to provide high sensitivity spectral analysis.

Three control parameters were available experimentally, the master power P_m, the slave power S_s, and the detuning Δ, defined as the angular frequency difference between the slave and master lasers. Dynamical behaviors evidenced at low S_s could be recovered at higher S_s by increasing both P_m and Δ. Many dynamical states were observed by varying these controls, and the most common can be understood by examining Fig. 1. Figure 1(a) shows a false color plot of the ESA output for fixed P_m and S_s as Δ is varied by changing the master wavelength (λ_m). λ_m is plotted along the x axis, while the frequency is plotted along the y axis. Bright colors correspond to higher modulation powers and blue to the noise floor of our instrumentation. The dynamic range of our plot ranges from -75 dBm (blue) up to -15 dBm (dark red).

For very low master powers, we were unable to attain stable locking at any detuning; rather, we observed an enhancement of low frequency noise at the boundary between the locked and unlocked states. For sufficient P_m we found three distinct regions of behavior: (i) for both positive and negative Δ far from zero, the ESA displays a beating frequency indicating that the slave laser is unlocked from the master laser; this corresponds to regions 1 and 2 [labels from Fig. 1(b)]; (ii) a stable locking region, where the slave laser synchronizes with the master and operates single mode; this is region 3; (iii) a region of complex dynamics that occurs on only the positive Δ unlocking boundary. In this region, as P_m increases, we observed single (6S) and double excitable pulses (6D), random switching between a locked state and complex multipulse transient (6C), random switching between locked and unlocked states (5), and random switching between two locked states [not shown in Fig. 1(b)]. For the highest P_m available in our experiment, the laser transitioned directly from locked region 3 to unlocked region 2 without any observed instabilities.

An example of a single pulse, observed experimentally in region 6S, is shown in Fig. 2(a). The pulse shape was invariant over a wide range of parameters but the mean time between consecutive pulses depended strongly upon the detuning. Far from the unlocked boundary, these pulses occurred very rarely. The frequency of the pulses increased with λ_m until they become nearly periodic as the laser entered the unlocked state. Such a behavior is well described using the Adler equation in the presence of noise. In this system, a saddle-node bifurcation occurs on a limit cycle and the distance between the stable and unstable fixed points increases as the detuning decreases. Double pulses were observed in region 6D; examples are shown on Fig. 2(b). They displayed similar properties to single pulses except that these pulses become periodic at half the beating frequency as the laser entered the unlocked regime. Further increase of the detuning led to an inverse period-doubling bifurcation. Analyzing a time series of double pulses, we noted over 1000 double excitable pulses occurred without any single pulses. As a result, double pulses cannot be explained as consecutive single pulses triggered by noise but as a saddle-node bifurcation on a period two limit cycle. As P_m was increased, double pulses gave way to random switching between a locked state and complex multipulse transient. Such a behavior could be the result of either multipulse excitability with a complex transient or random switching between a steady state and a chaotic attractor. For even higher P_m we observed random switching between locked and unlocked states, region 5 in Fig. 1(b), and eventually switching between two locked states. An example of the random switching between a locked state and a limit cycle is shown in Fig. 2(c), with a zoom of the limit-cycle oscillations in Fig. 2(d).

The appearance of double excitable pulses and their unlocking at a period related to half the beating frequency is perhaps the most interesting feature observed. This indicates that a saddle-node bifurcation occurs on a double loop limit cycle similarly to that described in [13], although we observe single and double excitable pulses over a wide parameter space without encountering any

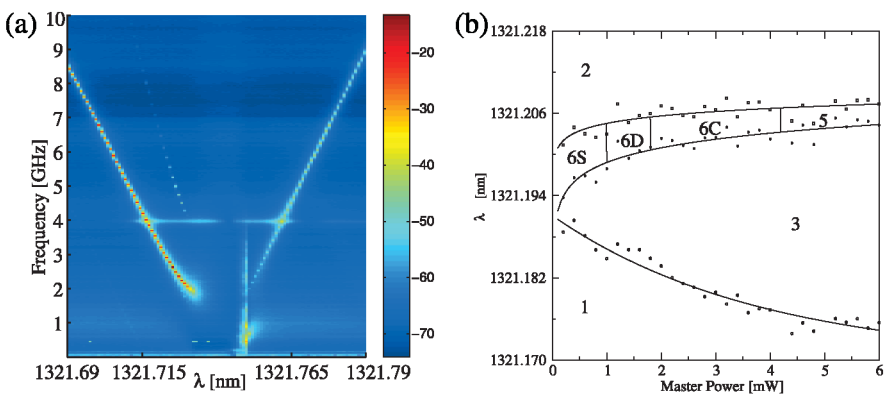

FIG. 1 (color). Experimental microwave mask (a) and parameter space mapping (b). Slave laser currents are 45 mA and 60 mA, respectively. Master power on left is 4 mW; fits on right are included as guides for the eye.

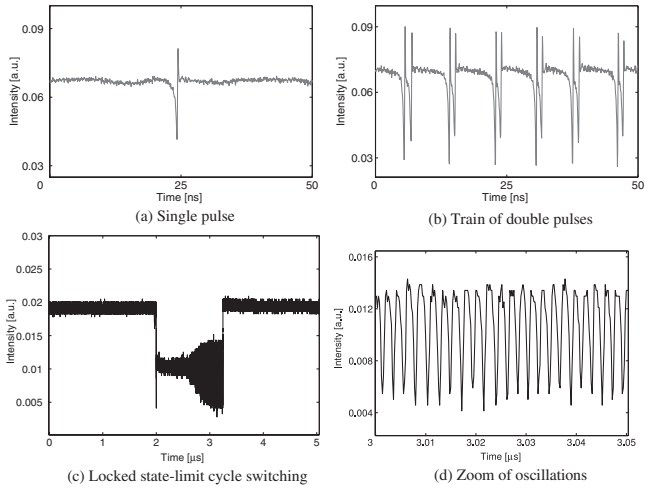

FIG. 2. Experimental single (a) and double (b) excitable intensity pulses. P_m is 3 mW and 4 mW, respectively; slave current is 80 mA, $\Delta = 9$ pm and 12 pm, respectively. Switching between locked state and limit cycle (c) with zoom of the limit cycle oscillations (d). P_m is 4 mW, slave current 45 mA, $\Delta = 9$ pm.

triple or quadruple pulses. We also observe that double pulses are associated with period two oscillations above the saddle-node line. A naive picture would suggest that the period-doubling bifurcation crosses the homoclinic bifurcation line but this is not possible in a codimension two bifurcation. For this reason, it is important to investigate the features of the model describing quantum dot semiconductor lasers with optical injection.

Theoretically, the dynamics of quantum dot lasers with optical injection can be described by rate equations for the complex amplitude of electric field E, the occupancy probability of the quantum dots ρ, and the carrier density in the surrounding quantum well, N_w [14]. The equations describing the dynamics read:

$$\dot{E} = \frac{1}{2} v_g g_0 \left(\frac{2\rho - 1}{1 + \epsilon |E|^2} - \frac{\gamma_s}{v_g g_0} \right) (1 + i\alpha) E + iE\Delta + \sqrt{\frac{\gamma_s^2}{\hbar\omega} S_m}$$

$$\dot{N}_w = -\gamma_N N_w + \frac{J}{q} - 2CN_w(1 - \rho)$$

$$\dot{\rho} = -\gamma_d \rho + CN_w(1 - \rho) - v_g \sigma \left(\frac{2\rho - 1}{1 + \epsilon |E|^2} \right) |E|^2. \qquad (1)$$

In these equations, the parameters are (numerical values used in the simulations presented in this Letter given in parentheses): γ_s (590 ns^{-1}) is the photon decay rate in the cavity, γ_N (1 ns^{-1}) and γ_d (1 ns^{-1}) the carrier decay rates in the quantum well and in the dot, respectively, C (1.02 ps^{-1}) is the capture rate from the quantum well into the dot, J (6.73×10^{-10} A) the current per dot, σ (0.6 nm^2) the interaction cross section of the carriers in the dot with the electric field, α (1.2) the linewidth enhancement factor, q the electronic charge, the detuning Δ is the angular frequency difference between the slave and master lasers, $|E|^2$ is the photon density, v_g (0.833×10^8 m/s) the group velocity, ϵ (2×10^{-22} m^3) the gain saturation coefficient, g_0 (72 cm^{-1}) the differential gain, ω (1.45 fs^{-1}) the master laser frequency, and S_m the energy density (J/m^3) in the master laser. When Δ and S_m are changed, the number and stability of the solutions of the dynamical system generally change as well.

The (S_m, Δ) parameter space of Eqs. (1) is represented in Fig. 3, showing qualitative agreement with the experimental observations. Regions with different behaviors, calculated using AUTO [16], are marked following the notation used to describe the experiment. A Hopf bifurcation separates region 3 from 1 and region 3 from 2. A saddle-node bifurcation occurs at the boundary between regions 3 and 4, and in region 4, the laser output has two stable steady state solutions corresponding to two locked states of different output powers and one saddle point. In this region one can observe bistability and in the presence of noise, random switching between the two locked states. A Hopf bifurcation separates regions 4 and 5 and the two stable attractors of region 5 are a limit cycle associated with an unlocked state and a fixed point associated with a locked state. In the presence of noise the laser will randomly switch between a lower power oscillatory state and a higher power stable state. As the injection power decreases, the stable limit cycle of region 5 goes through a sequence of bifurcations resulting in the complex behavior of region 6. A full description of this region is beyond the scope of this Letter but we will discuss in some detail the origin of the excitable pulsing behavior seen there.

A portion of region 6 close to the origin is presented in Fig. 4. The major features of the space are the saddle-node (SN) and the homoclinic (h^1) bifurcation curves. SN and h^1 are coincident except for the range between points B1 and B2 where h^1 goes through noncentral codimension two bifurcations and leaves the saddle-node curve forming a

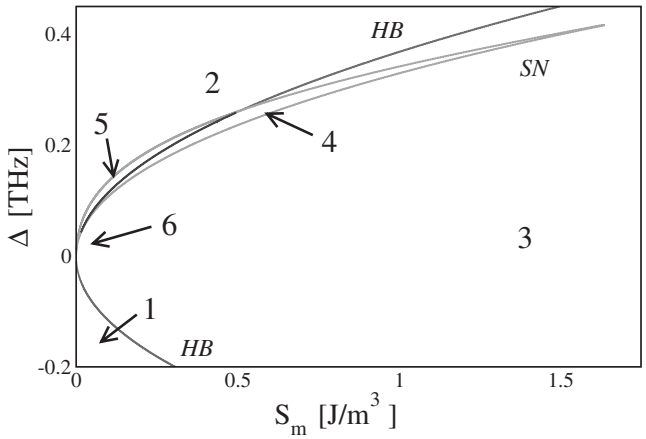

FIG. 3. (S_m, Δ) parameter space of Eqs. (1). The master power is plotted along the x axis and the detuning along the y axis. Regions 1 and 2 are unlocked; region 3 is stably locked; region 4 is bistable between two fixed points of different phase; region 5 is bistable between a stable fixed point and a limit cycle; in region 6 the laser exhibits excitable pulsing.

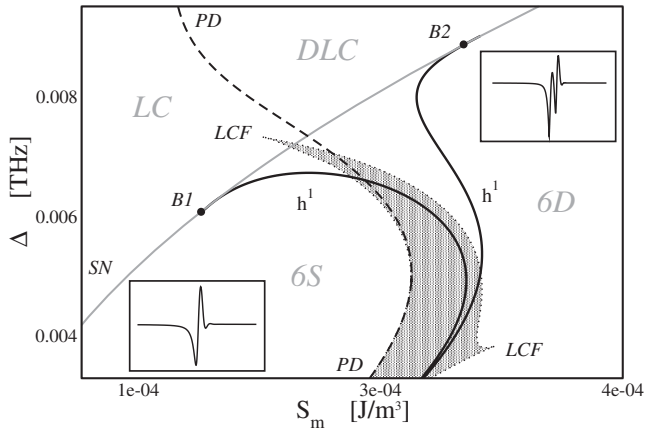

FIG. 4. Parameter space mapping of part of region 6 exhibiting excitable pulses. Single excitable pulses are found in region 6S; double excitable pulses are found in 6D. The regions above SN contain stable limit cycle (LC) and stable double limit cycles (DLC). A period-doubling line (PD) separates LC from DLC. The shaded set is bounded by limit-cycle fold-bifurcation boundary LCF. Numerically obtained single and double pulses are inset in regions 6S and 6D, respectively.

homoclinic tooth [13]. The stable limit cycle in region LC loses stability on the period-doubling curve (PD) giving rise to a stable double limit cycle in region DLC. When crossing from region LC to region 6S through h^1, the stable limit cycle undergoes a homoclinic bifurcation resulting in a pair of stable and unstable points connected by long and short heteroclines. Here, noise can induce the system to jump from the stable steady state to the vicinity of an unstable one, which results in a phase space excursion along the long heteroclinic trajectory that is shaped like a ''just broken'' limit cycle. In a similar fashion, when passing from region DLC to region 6D, the double limit cycle is broken and the system can be induced by noise to traverse the long heteroclinic trajectory shaped like a double limit cycle. It is interesting that both single- and double-pulse behavior happens on the *same 1-homoclinic bifurcation curve* h^1. As we follow h^1 we see a continuous deformation of the single-pulse shape observed around B1 to the double-pulse shape observed around B2. Figure 4 explains how the regions of single and double pulses coexist with h^1. Since PD cannot cross h^1 in a codimension two bifurcation point, two things happen. First, h^1 must leave the saddle-node curve at points B1 and B2 forming a homoclinic tooth. Second, along the boundary LCF of the shaded set a stable cycle undergoes a fold bifurcation, which creates a region of multistability with additional stable and unstable cycles. Inside the shaded region one of the stable cycles undergoes period doubling on the curve PD, while the other becomes 1-homoclinic on h^1 forming part of the tooth. Thus bifurcations at the crossing of PD and h^1 curves are spatially resolved. The homoclinic tooth crosses the Shilnikov line at two Belyakov points leading to the formation of n-homoclinics and multipulse excitability as suggested in [13]. The region in parameter space where this behavior is numerically observed is very narrow and has not been seen experimentally. The homoclinic tooth in the Fig. 4 is the only closed tooth observed in the system, and the single- and double-pulse scenarios described above are stable with respect to parameter changes.

In conclusion, we have experimentally observed the appearance of single and double excitable pulses in a quantum dot semiconductor laser with optical injection, the first such report of which we are aware. The presence of double excitable pulses can be associated with the appearance of period two oscillations in the unlocked region both experimentally and theoretically. Our theoretical analysis shows a clear and simple bifurcation scenario which enables the observation of single and double excitable pulses. It would be worthwhile to find a simpler model which exhibits similar features.

The authors wish to acknowledge funding from Science Foundation Ireland under Contract No. sfi/01/fi/co, the Research Frontiers program, Embark under the IRCSET scheme, and the PRTLI program of HEA.

[1] A. Pikovsky, M. Rosenblum, and J. Kurths, *Synchronization, A Universal Concept in Nonlinear Sciences* (Cambridge University Press, Cambridge, England, 2001).
[2] R. Adler, Proc. IEEE **61**, 1380 (1973).
[3] A. L. Hodgkin and A. F. Huxley, J. Physiol. **117**, 500 (1952).
[4] R. FitzHugh, Bull. Math. Biophys. **17**, 257 (1955); F. Brink *et al.*, Ann. N.Y. Acad. Sci. **47**, 457 (1946); A. T. Winfree, *The Geometry of Biological Time* (Springer, New York, 1980).
[5] F. Plaza, M. G. Velarde, F. T. Arecchi, S. Boccaletti, M. Ciofini, and R. Meucci, Europhys. Lett. **38**, 85 (1997).
[6] M. Giudici, C. Green, G. Giacomelli, U. Nespolo, and J. R. Tredicce, Phys. Rev. E **55**, 6414 (1997).
[7] H. J. Wünsche, O. Brox, M. Radziunas, and F. Heneberger, Phys. Rev. Lett. **88**, 023901 (2001).
[8] L. A. Lugiato, in *Progress in Optics*, edited by E. Wolf (North-Holland, Amsterdam, 1984), Vol. XXI, p. 69.
[9] L. Chrostowski *et al.*, IEEE Photonics Technol. Lett. **18**, 367 (2006).
[10] S. Barland *et al.*, Nature (London) **419**, 699 (2002).
[11] S. Wieczorek, B. Krauskopf, T. B. Simpson, and D. Lenstra, Phys. Rep. **416**, 1 (2005).
[12] P. Coullet, D. Daboussy, and J. R. Tredicce, Phys. Rev. E **58**, 5347 (1998).
[13] S. Wieczorek, B. Krauskopf, and D. Lenstra, Phys. Rev. Lett. **88**, 063901 (2002).
[14] D. O'Brien, S. P. Hegarty, G. Huyet, and A. V. Uskov, Opt. Lett. **29**, 1072 (2004).
[15] J. Muszalski, J. Houlihan, G. Huyet, and B. Corbett, Electron. Lett. **40**, 428 (2004).
[16] E. Doedel, T. Fairgrieve, B. Sandstede, A. Champneys, Yu. Kuznetsov, and X. Wang, Auto 2000, http://indy.cs.concordia.ca/auto continuation software used for Fig. 3 and 4.